

See discussions, stats, and author profiles for this publication at: <https://www.researchgate.net/publication/312561521>

Coarse-to-Fine Stacked Fully Convolutional Nets for lymph node segmentation in ultrasound images

Conference Paper · December 2016

DOI: 10.1109/BIBM.2016.7822557

CITATIONS

9

READS

254

5 authors, including:



Yizhe Zhang

University of Notre Dame

20 PUBLICATIONS 196 CITATIONS

[SEE PROFILE](#)



Michael Ying

The Hong Kong Polytechnic University

128 PUBLICATIONS 2,838 CITATIONS

[SEE PROFILE](#)



Lin Yang

University of Notre Dame

30 PUBLICATIONS 170 CITATIONS

[SEE PROFILE](#)

Some of the authors of this publication are also working on these related projects:



Brain Imaging [View project](#)



Microfluidic and imaging [View project](#)

Coarse-to-Fine Stacked Fully Convolutional Nets for Lymph Node Segmentation in Ultrasound Images

Yizhe Zhang*, Michael T. C. Ying†, Lin Yang*, Anil T. Ahuja‡, Danny Z. Chen*

*Department of Computer Science and Engineering, University of Notre Dame, Notre Dame, IN 46556, USA

Email: yzhang29@nd.edu, lyang5@nd.edu, dchen@nd.edu

†Department of Health Technology and Informatics, The Hong Kong Polytechnic University, Hung Hom, Hong Kong

Email: michael.ying@polyu.edu.hk

‡Department of Imaging and Interventional Radiology,

The Chinese University of Hong Kong, Prince of Wales Hospital, Shatin, NT, Hong Kong

Email: aniltahuja@cuhk.edu.hk

Abstract—Ultrasound as a well-established imaging modality is widely used in imaging lymph nodes for clinical diagnosis and disease analysis. Quantitative analysis of lymph node features, morphology, and relations can provide valuable information for diagnosis and immune system studies. For such analysis, it is necessary to first accurately segment the lymph node areas in ultrasound images. In this paper, we develop a new deep learning method, called Coarse-to-Fine Stacked Fully Convolutional Nets (CFS-FCN), for automatically segmenting lymph nodes in ultrasound images. Our method consists of multiple stages of FCN modules. We train the CFS-FCN model to learn the segmentation knowledge from a coarse-to-fine, simple-to-complex manner. A data set of 80 ultrasound images containing both normal and diseased lymph nodes is used in our experiments, which show that our method considerably outperforms the state-of-the-art deep learning methods for lymph node segmentation.

I. INTRODUCTION

Lymph nodes are found throughout human body including the neck, armpit, and stomach. They are major sites for immune cells and are important for immune system functions. Ultrasound is widely used in imaging lymph nodes for clinical diagnosis. It is a common first-line imaging examination for patients presented with neck lumps since it is non-invasive and commonly available in hospitals. Quantitative analysis of lymph nodes' size, shape, morphology and their relations in ultrasound images gives useful and reliable information for clinical diagnosis, cancer staging, patient prognosis, and treatment planning. It also helps obtain a better understanding of what are solid and effective features for diagnosing lymph node related diseases. An automatic method for segmenting lymph nodes in ultrasound images lays a foundation for such quantitative analysis and disease studies.

An ultrasound image can contain multiple lymph nodes. Some lymph node areas can be unclear to view and their borders are blurred (see Fig. 1). Also, many non-lymph node areas can be visually very similar to lymph nodes (e.g., the green areas in Fig. 1). Thus, it is a non-trivial task to accurately segment and detect lymph nodes in ultrasound images.

Some previous work was done on lymph node segmentation in ultrasound images. A texture enhanced graph cut based method was developed for ultrasound image segmentation [16]; although this method preserves object boundaries better than the pure intensity level based graph cut method, it gives

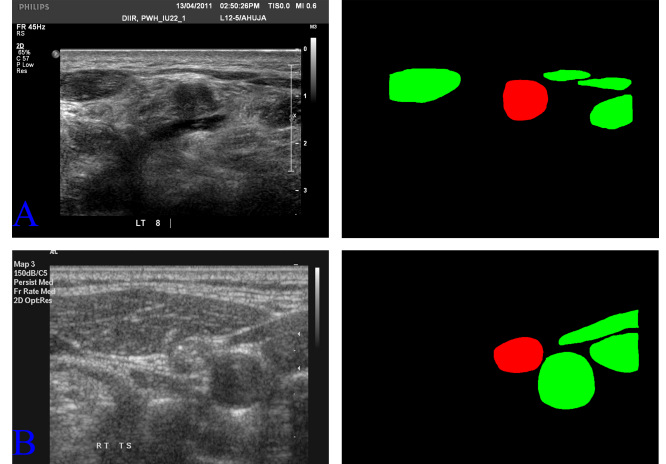


Fig. 1: Examples for difficult cases. Left column: input images; right column: red objects are real lymph nodes, and green areas are objects seemingly like lymph nodes (but are actually not).

only a set of proposal regions as final output and does not address detection of lymph node locations (i.e., which areas are lymph nodes). An elliptical shape prior was designed to help determine more accurate lymph node borders [13]; but similar to [16], it also did not address the detection problem — a manually delineated bounding box is required as part of the input to cover each lymph node in the images. Computer-aided diagnosis (CAD) systems for sonographic assessment of lymph nodes were reported [2], [6], [8], [10], [11], [12], [14]; similar to [13], [16], these systems could not perform fully automated sonogram segmentation of lymph nodes. Instead, manual delineation of lymph nodes in sonograms is needed. A C-means algorithm was used to cluster pixels into different categories [15], which utilizes only pixel-level intensity values. Since lymph node areas can be in dark or bright conditions, and non-lymph node objects (e.g., blood vessels and background tissues) can also contain dark or bright areas, using only pixel-level intensity cannot ensure satisfactory results. In summary, all the previous related work either has no detection part and requires manual delineation, or the detection methods (based on intensity level) are too simple to give accurate results.

Recently, deep learning methods emerged as powerful tools

for semantic segmentation tasks. Region based convolutional neural networks (R-CNN) [3] performed segmentation with CNN using proposal regions. Its main advantages are: (1) it is relatively scale-free (the generated proposal regions can be of arbitrary sizes; as CNN is trained on such proposal regions, it can handle objects of different scales); (2) it avoids a dense window sliding approach and reduces a significant amount of training and testing time. Fully convolutional networks (FCN) [5] also showed promising segmentation results. Different from R-CNN, FCN is a window-based method, and several FCN models were given for different segmentation tasks. For example, U-Net [7] is an FCN model for biomedical imaging tasks; it systematically combines the fine imaging details with middle-level and object-level information for accurate object detection and segmentation in biomedical images. CUMedNet [1] is also an FCN model for biomedical image segmentation. Comparing to the U-Net model, CUMedNet has a smaller model size and uses some auxiliary classifiers in training.

U-Net [7] and CUMedNet [1] are two state-of-the-art deep learning models for biomedical image segmentation and are directly applicable to our problem. However, as discussed above, segmenting and detecting lymph nodes in ultrasound images can be difficult for non-experts, and only well-trained sonographers can confidently determine the locations of lymph nodes in ultrasound images. How well these models can gain expert-level knowledge remains unclear. In this paper, we explore this issue by studying these models. Further, we propose a new coarse-to-fine stacked FCN model (CFS-FCN) that is designed to incrementally learn segmentation knowledge from the non-expert level to expert level for lymph node segmentation. Our model has two stages, each stage consisting of one FCN module. The first FCN module is trained to transform a raw input image to a segmentation label map (the intermediate result) which shows all the areas visually similar to lymph nodes (non-expert decision). Then, the second FCN is trained to use the intermediate result combined with the raw image to produce the final (real) lymph node segmentation label map. The whole system learns segmentation (filtering) knowledge in a coarse-to-fine, simple-to-complex manner. In addition to our proposed CFS-FCN model, as a post-processing step, we further apply a convex-shape constraint based graph search method to improve the lymph node boundary accuracy of the segmentation results.

Our model makes several contributions for semantic segmentation in biomedical images.

1. We introduce a multi-stage incremental learning concept for designing deep learning models. Based on this concept, the deep learning model learns segmentation knowledge in a coarse-to-fine, simple-to-complex manner.

2. A small-size FCN is used to build every FCN module. In each learning stage, the model is not too complicated, and this can help avoid over-fitting in each learning stage. Since the label maps are designed in an incremental manner (coarse-to-fine), the over-fitting risk for the whole model is greatly reduced.

3. Three different training strategies for training CFS-FCN are proposed and investigated.

In our experiments, 80 ultrasound images that contain reactive, metastasis and lymphoma lymph nodes are used to

evaluate the segmentation performance of different models and training strategies. The experimental results show that our method outperforms the state-of-the-art deep learning methods for lymph node segmentation in ultrasound images by 4% in mean IU (intersection over union) and 5% in F1 score. Our model can learn difficult biomedical image segmentation knowledge better than previous deep learning models.

II. METHOD

A. Overview

Our CFS-FCN model consists of multiple stages of FCNs (fully convolutional networks). An overview of CFS-FCN is given in Fig. 2. FCN *A* is trained to learn segmentation (filtering) knowledge from the raw input image to produce a segmentation label map (intermediate result) that shows all the areas visually similar to lymph nodes (non-expert knowledge, possibly with false positives). Then FCN *B* is trained to use the intermediate result combined with the raw image to produce the final (real) lymph node segmentation.

Our model can be extended to have more than 2 stages. The number of stages used depends on different applications. There are three main design issues to this model: (i) The architecture of FCN modules (FCN *A* and FCN *B*); (ii) the coarse-to-fine label maps (the intermediate label map and final label map); (iii) a suitable training strategy for training CFS-FCN. The following Subsections *B*, *C*, and *D* explore these three issues, respectively. In Subsection *E*, a post-processing is applied to further refine the lymph node boundaries based on the segmentation results produced by CFS-FCN.

B. FCN module

Fully convolutional network (FCN) is a deep learning model that mainly contains convolutional layers and does not contain any fully connected layer. For semantic segmentation on a 2D image I , the input of FCN is an $n \times m \times c$ tensor, where n is the length of I , m is the width of I , and c is the number of channels (for a color image, $c = 3$; for an intensity image, $c = 1$). The output of FCN is usually an $n \times m \times s$ tensor, where s is the number of object classes in the segmentation task. For example, for a pixel with coordinates (x, y) , if it belongs to class #1, then $(x, y, 1)$ in the output tensor should have a very large value (close to 1), and (x, y, i) , $i = 2, \dots, s$, should all have low values (close to 0). In our model, for the intermediate label map, there are two classes: (1) objects visually similar to lymph nodes; (2) objects visually unlike lymph nodes. For the final label map, there are two classes: (1) objects that are real lymph nodes; (2) other tissue areas and background.

Fig. 3 shows the detailed FCN architecture in our model. There are two main design issues to the FCN module. (a) Making the model deeper (with more max-pooling layers) can help the model capture larger-scale object-level information. One 2x2 max-pooling operation reduces the image size to 1/4 of its original size. It allows the corresponding masks in the convolutional layers to work on a larger view in the image domain. This operation is essential for the model to capture object-parts-level and whole-object-level image cues. (b) Fusing (element-wise addition) the segmentation results up-convoluted from different scales is essential for more accurate lymph node segmentation. Since the lymph node sizes can vary

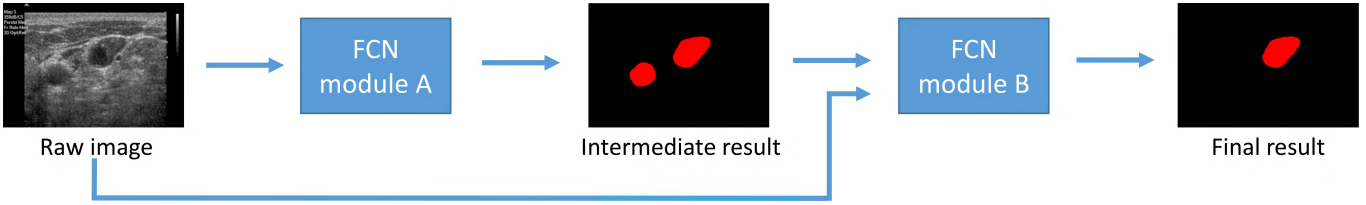


Fig. 2: Overview of our proposed coarse-to-fine stacked FCN model: FCN module A first takes the raw input image and produces intermediate segmentation results for objects that look like lymph nodes; FCN module B then works on the intermediate segmentation result with a reference of the raw image to generate the final lymph node segmentation.

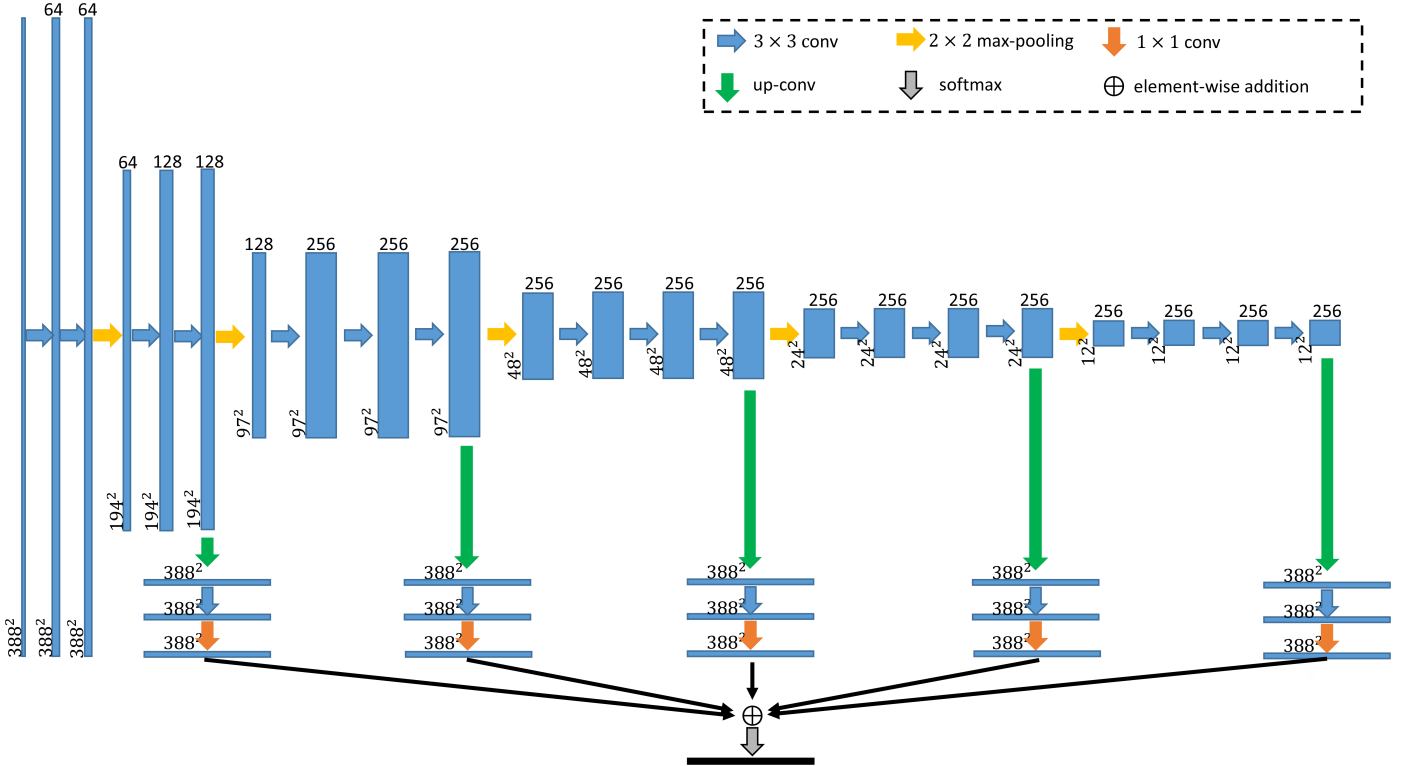


Fig. 3: The architecture of the FCN module. The input of FCN A is a $388 \times 388 \times 1$ tensor (raw intensity image). The input of FCN B combines the output of FCN A (a $388 \times 388 \times 2$ tensor) and the raw intensity image (a $388 \times 388 \times 1$ tensor). The input of FCN B is a $388 \times 388 \times 3$ tensor. Despite the input layer, FCN A and FCN B have the same architecture as shown above.

considerably in the images, fusing the output from different scales helps the final results capture lymph nodes of different sizes. Our FCN module architecture is similar to that in [1]; but different from [1], we do not use auxiliary classifiers on the output up-convolved from all the scales.

C. Coarse-to-fine label maps

The sequence of the label maps is essential to the success of our stacked FCNs. It is natural to make the label maps from coarse to fine, simple to complex (see Fig. 4). Our model has two FCN modules. FCN A predicts areas that look like lymph nodes (maybe not real lymph nodes), and FCN B further refines the intermediate results to generate the final (real) lymph node segmentation. For FCN B, the raw image is also part of its input as a reference for the refinement.

We let a non-expert label all possible lymph node areas

in our images. These intermediate label maps are expected to cover all true lymph nodes, and may contain false positives (see Fig. 4). These label maps are used to guide the training of FCN A. For FCN B, the label maps show the real lymph node areas and are marked by an experienced sonographer. In case the intermediate label maps miss some real lymph nodes, we generate the intermediate label maps by merging the intermediate label maps and the final label maps.

D. Training stacked FCNs

After defining the model architecture, we use image samples and their corresponding label maps to learn the parameter values of the CFS-FCN model. We denote FCN A as F_A and FCN B as F_B . For training, we use k images x_j , $j = 1, 2, \dots, k$; their intermediate label maps are y_j^A , $j = 1, 2, \dots, k$; the final label maps are y_j^B , $j = 1, 2, \dots, k$.

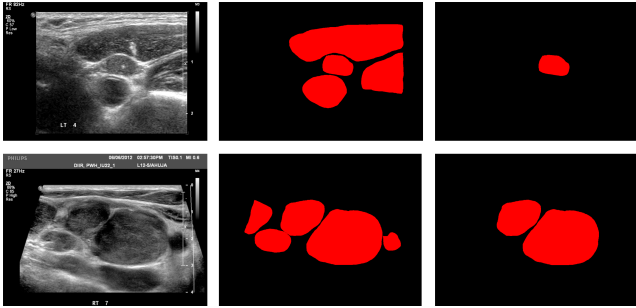


Fig. 4: Left column: input images; middle column: intermediate label maps (marked by a non-expert, the desired output of FCN A); right column: final label maps (marked by an experienced sonographer, the desired output of FCN B).

A stochastic gradient descent based method (e.g., Adam [4] or RMSProp [9]) can be applied to train our model. In experiments, we choose to use the Adam optimizer. Adam optimizer is known that it can yield quicker convergence in training deep network. Besides choosing the optimizer, there are different options for training a multi-stage model. Strategy I: train F_A and F_B at the same time using the same image data; both modules have influence to each other in the training. Strategy II: train F_A using only the intermediate label maps, and train F_B using only the final label maps; F_A has influence to F_B , but the final label maps and F_B have no influence to F_A . Strategy III: first train F_A using the intermediate label maps, and then fix F_A and train F_B . Similar to Strategy II, F_A has influence to F_B , but not vice versa. Different from Strategy II, the influence from F_A to F_B remains the same for the same image samples in different epochs (since F_A has been trained and is fixed).

It is not trivial to decide which training strategy is better. Intuitively, Strategy I lets the influence between F_A and F_B go in both ways, and may produce a more robust multi-stage model. On the other hand, Strategies II and III emphasize the order relation between F_A and F_B in training, and the whole model might be easier to be trained. In experiments, we tested all three strategies and found that Strategy I (Fig. 5) works better.

E. Boundary refinement

After obtaining the final segmentation results from the CFS-FCN model, we noticed that some border contours of the lymph nodes can be fuzzy or irregular. Thus, we apply a post-processing to further refine the lymph node boundaries based on the segmentation results of CFS-FCN.

We observed that most of the time, a lymph node is a convex-shape object in ultrasound images. Although possible, it is not very common to find concave points on the border of a lymph node. Thus, we think using a soft convex-shape constraint to refine the border contours of lymph nodes will help generate more accurate lymph node segmentation.

We model this contour optimization problem as a shortest path problem on a graph. Given a contour C for a lymph node segmented by CFS-FCN, we uniformly sample g points on C clockwise in the input image. For each sample point a_j , let r_j

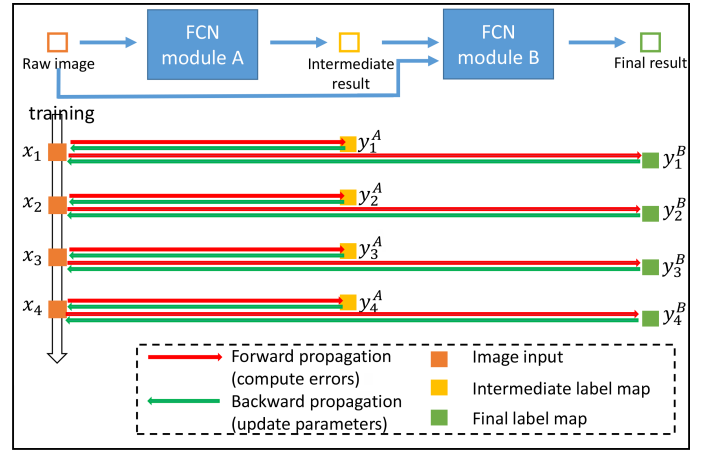


Fig. 5: Training Strategy I: For each training sample, the intermediate label map is first used to compute the output errors for F_A (forward propagation) and update F_A (backward propagation); then the final label map is used to compute the output errors for F_B and update both F_B and F_A .

be a ray of h pixels orthogonal to the direction of the curvature of C at a_j (r_j centers at $a_j \in C$). Denote the i -th point (pixel) on the ray r_j as $p_i^j = (x_{p_i^j}, y_{p_i^j})$ in the image. To ensure the optimized output contour C' being sufficiently smooth, we apply a *smoothness constraint*, specified by a parameter s : Each p_i^j is allowed to connect only to $p_{i'}^{j+1} - [j/g] \times g$ along C' , for any $|i' - i| \leq s$, $i = 1, 2, \dots, h$, $i' = 1, 2, \dots, h$, and $j = 1, 2, \dots, g$ (we choose $s = 5$). We also enforce the *shape convexity constraint*: Any concave edge-to-edge connection ($p_i^{j-1} p_i^j$ to $p_{i'}^{j+1} p_{i''}^{j+1}$) along C' is penalized by incurring a large connection cost. A graph G is then built on the sample points (graph nodes) of these rays with node weights reflecting inverse image gradient responses and edge weights reflecting the degrees of convexity at the internal angles of the sought contour C' . A parameter w is used to control the relative importance between the node weights and edge weights in G . Computing the optimal convex-shape constrained closed contour C' in G takes totally $O(s^3 h^2 g)$ time. More details of this algorithm are given in the full paper. Our experiments show that this boundary refinement process produces a cleaner and more accurate lymph node segmentation.

III. EXPERIMENTS

We collected 80 ultrasound images each containing one or more lymph nodes. There are three different types of lymph nodes in the images: reactive, metastasis, and lymphoma lymph nodes. There are quite large variations in size and appearance among the lymph nodes in the images. It is thus a challenging data set for automatic lymph node segmentation.

A two-fold cross validation scheme is used to test different models for lymph node segmentation. We randomly split all the images into two folders with equal size. To test one model, we first use images in folder 1 to train the model, and then test the model's performance using images in folder 2. We repeat the above process by switching the roles of folder 1 and folder 2. We apply the commonly used mean IU (intersection over

union) and F1 score metrics to show the performance of each model.

In more detail, suppose there are k images x_1, x_2, \dots, x_k , and a model produces predicted label maps y_1, y_2, \dots, y_k . There are two classes in this segmentation task: (1) lymph node areas; (2) other tissue areas and background. Suppose the number of correctly predicted pixels for lymph nodes (TP for lymph nodes) is n_{11} , the number of wrongly predicted pixels for lymph nodes (FP for lymph nodes) is n_{12} , the number of wrongly not predicted pixels for lymph nodes (FN for lymph nodes) is n_{21} , and the number of correctly predicted pixels for other tissue areas and background is n_{22} .

The IU for class 1 is $n_{11}/(n_{11} + n_{12} + n_{21})$. The IU for class 2 is $n_{22}/(n_{22} + n_{21} + n_{12})$. The mean IU is the average of these two classes.

The F1 score is calculated as:

$$\text{Precision} = n_{11}/(n_{11} + n_{12}), \text{Recall} = n_{11}/(n_{11} + n_{21})$$

$$\text{F1 score} = 2(\text{Precision} \times \text{Recall})/(\text{Precision} + \text{Recall})$$

U-Net [7] and CUMedNet [1] are two state-of-the-art deep learning models for biomedical image segmentation. We directly compare our CFS-FCN model (with three different training strategies) to these two models. To evaluate the effectiveness of our multi-stage incremental learning approach comparing to a simpler one-shot learning approach, we also test a naive stacked FCN model with the same size and architecture as CFS-FCN but with no intermediate supervision.

A desktop computer with 32GB memory and an Nvidia TITAN X graphics card (12 GB graphics memory) is used for our experiments. Torch is the software platform for implementing U-Net, CUMedNet, and our model. For the Adam optimizer, the learning rate is set as 0.000005, and all other parameters use the default settings. All the images used in the experiments are first resized to 388×388 . For the post-processing, since we only want the contour search method to work in a narrow band around the contour of each lymph node segmented by CFS-FCN, we set $h = 10$, $s = 5$, $g = 360$, and $w = 1$.

Fig. 6 and Fig. 7 show the testing mean IU and testing F1 scores for different deep learning models and training strategies. The best performance of each model (its memory cost on the graphics card in training and the effectiveness) are shown in Table I. Our CFS-FCN model with training Strategy I performs the best and is considerably better than U-Net [7] and CUMedNet [1]. The naive stacked FCN that has the same model complexity as our CFS-FCN model but does not use intermediate supervision in training performs much worse than CFS-FCN. This shows that the better performance of CFS-FCN is mainly due to our new coarse-to-fine learning approach. Simply increasing the complexity of a model without a more judicious design may make the model (e.g., the naive stacked FCN) overfit the training data and perform worse on testing data. Fig. 8 shows some visual comparison segmentation examples. Our method is considerably better in detecting and segmenting true lymph nodes in ultrasound images. The last column in Fig. 8 shows that boundary refinement (BR) can help obtain convex objects in the segmentation results.

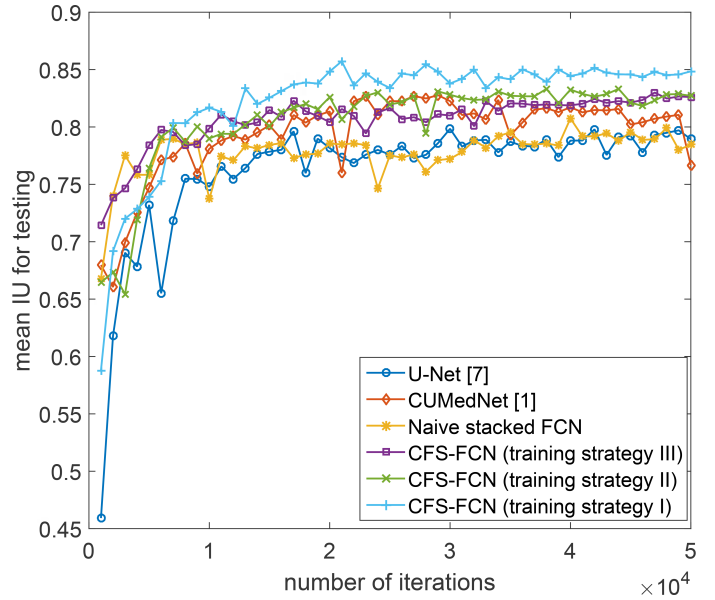


Fig. 6: The mean IU testing performance for every model with respect to the number of iterations used in training.

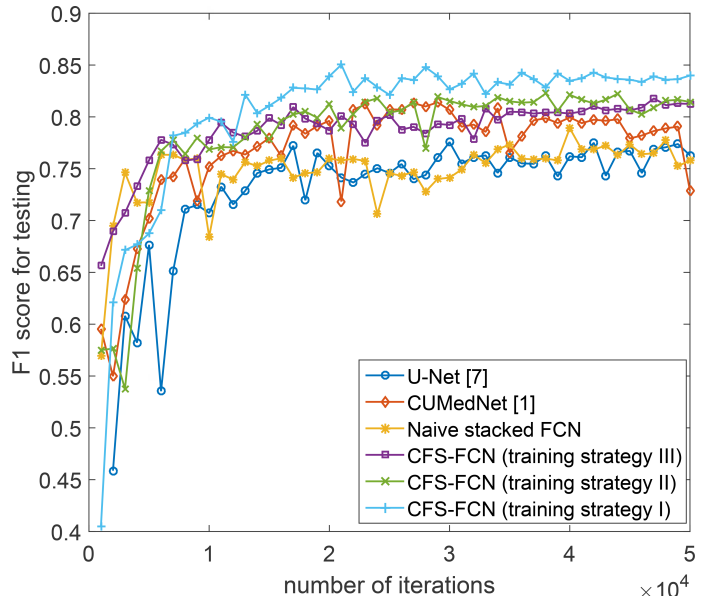


Fig. 7: The F1 score testing performance for every model with respect to the number of iterations used in training.

IV. CONCLUSIONS

In this paper, we proposed a novel coarse-to-fine stacked FCN (CFS-FCN) deep learning model for lymph node segmentation in ultrasound images. We designed our new model to learn segmentation knowledge in a coarse-to-fine and simple-to-complex manner. Comparing to the state-of-the-art deep learning methods for biomedical segmentation, our method yields better segmentation of lymph nodes in ultrasound images. We further applied a convex-shape constraint based boundary refinement method to enhance the quality of the segmented lymph nodes. With accurately detected and segmented

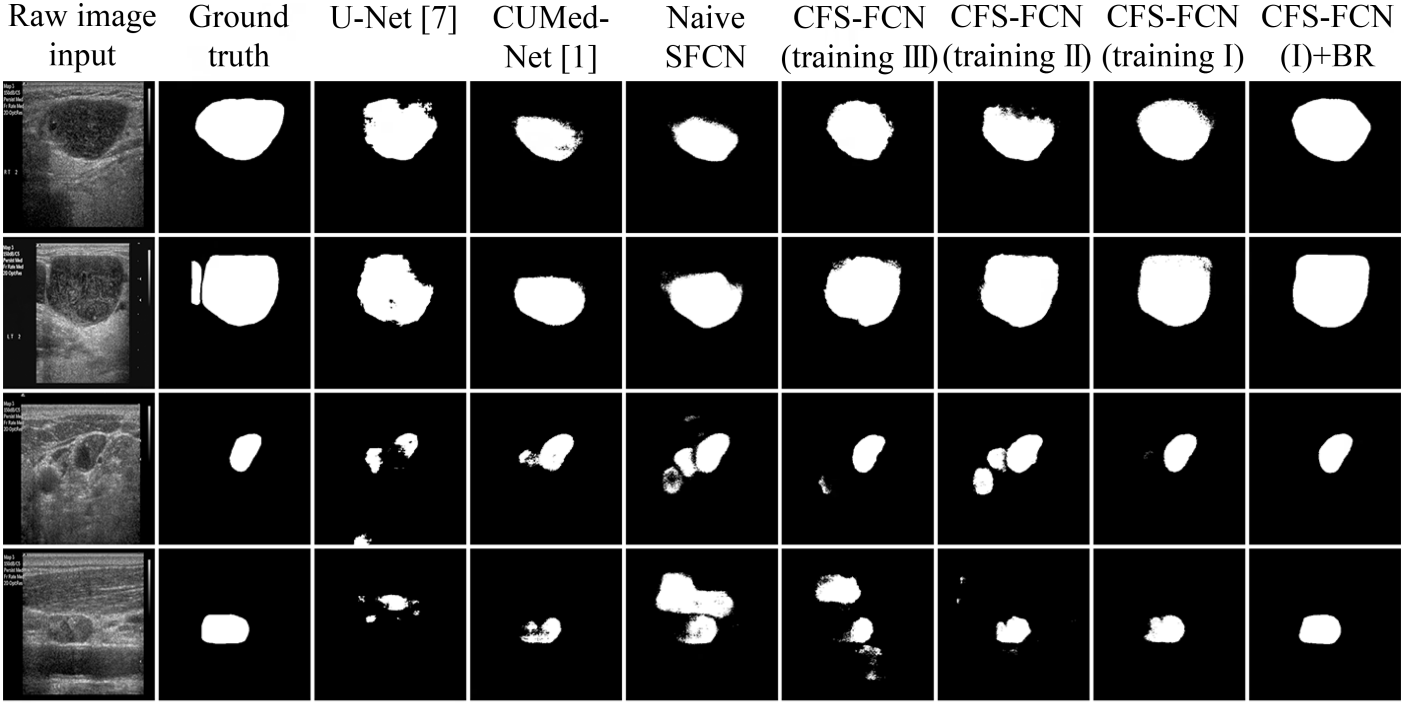


Fig. 8: Some visual segmentation results of different models (BR is for boundary refinement).

	Mean IU	F1 score	Memory cost
U-Net [7]	0.798	0.775	~5200 MB
CUMedNet [1]	0.816	0.798	~950 MB
Naive stacked FCN	0.799	0.778	~1920 MB
CFS-FCN (training strategy III)	0.830	0.818	~1920 MB
CFS-FCN (training strategy II)	0.833	0.822	~1920 MB
CFS-FCN (training strategy I)	0.851	0.843	~1920 MB
CFS-FCN (training strategy I) + BR	0.860	0.858	~1920 MB

TABLE I: The best performance of each model after having been trained relatively stably (> 40000 iterations) and its memory cost on the graphics card in training (BR is for boundary refinement).

lymph nodes, quantitative measurement and analysis can be developed for computer-aided diagnosis and studies of lymph node related diseases using ultrasound images.

V. ACKNOWLEDGMENT

This research was supported in part by NSF under Grants CCF-1217906 and CCF-1617735.

REFERENCES

- [1] H. Chen, X. J. Qi, J. Z. Cheng, and P. A. Heng. Deep contextual networks for neuronal structure segmentation. In *30th AAAI Conference on Artificial Intelligence*, 2016.
- [2] A. Chmielewski, P. Dufort, and A. M. Scaranello. A computerized system to assess axillary lymph node malignancy from sonographic images. *Ultrasound in Medicine & Biology*, 41(10):2690–2699, 2015.
- [3] R. Girshick, J. Donahue, T. Darrell, and J. Malik. Rich feature hierarchies for accurate object detection and semantic segmentation. In *CVPR*, pages 580–587, 2014.
- [4] D. Kingma and J. Ba. Adam: A method for stochastic optimization. *arXiv preprint arXiv:1412.6980*, 2014.
- [5] J. Long, E. Shelhamer, and T. Darrell. Fully convolutional networks for semantic segmentation. In *CVPR*, pages 3431–3440, 2015.
- [6] D. E. Loren, C. M. Seghal, G. G. Ginsberg, and M. L. Kochman. Computer-assisted analysis of lymph nodes detected by EUS in patients with esophageal carcinoma. *Gastrointestinal Endoscopy*, 56(5):742–746, 2002.
- [7] O. Ronneberger, P. Fischer, and T. Brox. U-net: Convolutional networks for biomedical image segmentation. In *MICCAI, Part III*, pages 234–241, 2015.
- [8] S. Sammet, K. D. Evans, M. O. Irfanoglu, A. Strapp, and R. Machiraju. The feasibility of hybrid automatic segmentation of axillary lymph nodes from a 3-D sonogram. *Ultrasound in Medicine & Biology*, 37(12):2075–2085, 2011.
- [9] T. Tielemans and G. Hinton. Lecture 6.5-rmsprop, coursera: Neural networks for machine learning. Technical report, 2012.
- [10] J. Zhang, Y. Wang, Y. Dong, and Y. Wang. Sonographic feature extraction of cervical lymph nodes and its relationship with segmentation methods. *Journal of Ultrasound in Medicine*, 25(8):995–1008, 2006.
- [11] J. Zhang, Y. Wang, Y. Dong, and Y. Wang. Ultrasonographic feature selection and pattern classification for cervical lymph nodes using support vector machines. *Computer Methods and Programs in Biomedicine*, 88(1):75–84, 2007.
- [12] J. Zhang, Y. Wang, Y. Dong, and Y. Wang. Computer-aided diagnosis of cervical lymph nodes on ultrasonography. *Computers in Biology and Medicine*, 38(2):234–243, 2008.
- [13] J. Zhang, Y. Wang, and X. Shi. An improved graph cut segmentation method for cervical lymph nodes on sonograms and its relationship with node's shape assessment. *Computerized Medical Imaging and Graphics*, 33(8):602–607, 2009.
- [14] J. Zhang, Y. Wang, B. Yu, X. Shi, and Y. Zhang. Application of computer-aided diagnosis to the sonographic evaluation of cervical lymph nodes. *Ultrasonic Imaging*, 38(2):159–171, 2016.
- [15] Q. Zhang, C. Huang, C. Li, L. Yang, and W. Wang. Ultrasound image segmentation based on multi-scale fuzzy c-means and particle swarm optimization. In *International Conference on Information Science and Control Engineering*, pages 1–5, 2012.
- [16] C.-M. Zhy, G.-C. Gu, H.-B. Liu, J. Shen, and H. Yu. Segmentation of ultrasound image based on texture feature and graph cut. In *International Conference on Computer Science and Software Engineering*, pages 795–798, 2008.